

Light Scattering and Size Exclusion Chromatography (SEC) in Biopharma

Author

Moritz Susewind
Agilent Technologies, Inc.

Introduction

Detection based on the principle of light scattering with size exclusion chromatography (SEC) is a powerful technique to identify molar mass and size distributions of synthetic polymers such as polystyrene (PS), polymethyl methacrylate (PMMA), polycarbonate (PC), and biopolymers. Especially the latter has received increased attention recently in the biopharmaceutical industry with applications including bioconjugates, proteins, monoclonal antibodies (mAbs), mRNA¹, viruses (adeno-associated viruses, AAVs), extracellular vesicles (EVs), and liposomal nanoparticles (LNPs).

SEC in biopolymer analyses

What is the reason to use SEC as a measure to fractionate complex polymer samples? Analysis based on SEC can both identify and quantify higher aggregates of biomolecules, of which further analyses can be done by elaborate light scattering equipment. With that information, quality control of biomolecules, including applications such as drug-to-antibody ratio (DAR) analysis of antibody drug conjugates (ADCs), can be done.² The strategy, to first separate molecules by size and then to analyze those single size fractions, leads to more precise results than measurements in batch.

Use of calibrants for determination of molecular weights in SEC

As SEC is a relative method in determination of molecular weight, calibration of the chromatographic columns is normally done with analytical standards consisting of narrowly distributed polymers, which are available for a broad range of analyte classes.³ Despite the universal applicability, a major drawback of this method is the lack of the primary information about size of the original molecules under investigation and, if a standard matching the polymer class is unavailable, accurate molar mass determination is not available.

Light scattering for direct measurement of physicochemical parameters

To circumvent the use of calibrants, analytical scientists rely on light scattering detectors to not only determine the weight average of molar mass (M_w) directly without needing to calibrate the chromatographic column, but also to obtain information about molecular size. The latter can be deduced in static light scattering (SLS) by the radius of gyration R_g and in dynamic light scattering (DLS) by the hydrodynamic radius R_H of the analytes. Also, based on the ratio of the two size expressions, it is possible to deduce the topology of the molecules, that is, if the polymer or polymer aggregate adapts the morphology of a homogeneous sphere, a hollow sphere, a random polymer coil, or something else.⁴ Alternatively, this topological information can also be extracted either by viscometry and a Mark-Houwink plot⁵ or by the R_g - M relation, which is analogous to the Mark-Houwink plot. Here, it can be stated that DLS provides a more robust and easy-to-handle system. It is important to note that both techniques, multi-angle (2 θ -angle) static light scattering and DLS, can be implemented simultaneously in SEC by consecutive coupling.

Theoretical and practical considerations of light scattering in biopharma

In this white paper, some theoretical and practical background paired with selected examples from biopharma is shown to exemplify the tremendous potential of light scattering as a detection method in SEC. Using light scattering, molar mass, size, and conformation of fractionated biomolecules under physiological conditions can be monitored online.

Static light scattering (SLS) in SEC

When incident light scatters with soft matter quasi-elastically (see Figure 1), the scattered light intensity is proportional to the weight average of molar mass M_w , the concentration c , and the scattering contrast factor K . The latter is the product of a constant $(4\pi^2)/N_L$, the refractive index of the solvent n_0^2 , the refractive index increment of the polymer in solution $(\delta n_p/\delta c)^2$, and the wavelength of the incident laser light λ^{-4} .

This applied to the screening of polymer-solvent interactions, referring to this fundamental equation (Equation 1) with A_2 , the second virial coefficient, it can easily be shown that by the sum of all scattering components it is possible to attain the weight average of molar mass M_w .

$$\frac{Kc}{R_\theta} = \frac{1}{M} + 2A_2c$$

Equation 1.

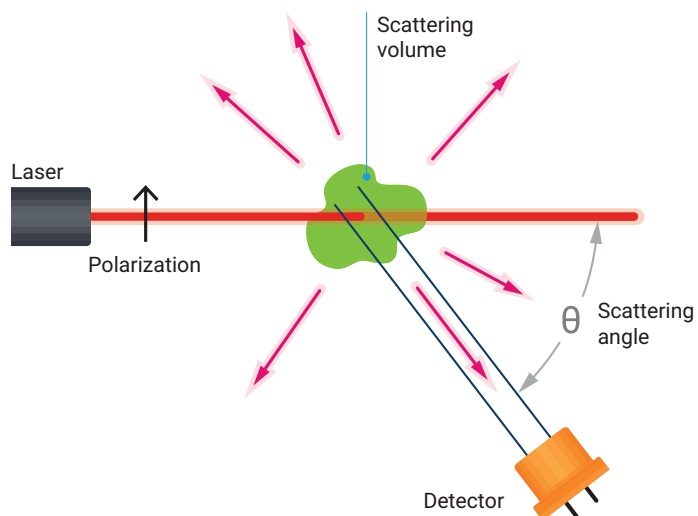


Figure 1. Scheme of a classical light scattering setup with scattering angle θ .

This simple term is only valid for isotropic scatterers (Rayleigh scattering). If molecules become larger than $d > \lambda/20$, interference of scattered light from more than a single scattering center lets us introduce the particle form factor $P(q)$. This means that the scattered light intensity becomes angle-dependent (see Figure 2).

Pair-wise summation of all scattering centers and introduction of a center of mass coordinate system leads us to a series expansion (Equation 2), which can be terminated for particles with a radius of gyration $R_g < 50$ nm.⁴

$$P(q) = 1 - \frac{R_g^2 q^2}{3} + \dots$$

Equation 2.

Replacing scattering vector q by the scattering angle θ and introducing polymer-solvent interactions by the second virial coefficient A_2 , we end up with the final static light scattering equation (Equation 3).

$$\frac{Kc}{R_\theta} = \frac{1}{Mw} \left[1 + \frac{16}{3} \frac{\pi^2 n_0^2}{\lambda^2} \langle R_g^2 \rangle_z \sin^2\left(\frac{\theta}{2}\right) \right] + 2A_2c$$

Equation 3.

Double extrapolation of term Kc/R_θ versus $\theta \rightarrow 0$ and $c \rightarrow 0$ according to Zimm yields the inverse weight average of molar mass. From the slope of Kc/R_θ versus θ , one gets the z-average of the radius of gyration squared and from the slope of the c-dependent linear extrapolation, the second virial coefficient.

In practice, software like the Agilent WinGPC Software is doing this analysis automatically for each slice in the chromatographic elugram when a multi-angle light scattering (MALS) detector has been used for data acquisition. So, for each chromatographic slice, Mw and R_g are determined from the angle-dependent scattering intensity plot by extrapolation of $\theta \rightarrow 0$. The reason for this limit is that particle form factor $P(q) \rightarrow 1$ means that scattering intensity becomes independent of particle size and shape. It should be mentioned though, that size determination is only valid above a lower limit of $R_g > 10$ nm, and molecular weight can also be determined for isotropic scatterers such as bovine serum albumin (BSA), which is often used as an isotropic standard molecule.

It is important to note that for polydisperse samples consisting of N_i species of molar mass M_i , one gets the z-average of the squared radius of gyration according to Equation 4.⁶

$$\langle R_g^2 \rangle_z = \frac{\sum_i w_i M_i \langle R_g^2 \rangle_i}{\sum_i w_i M_i}$$

Equation 4.

Thereby each species has its own mean squared radius of gyration over all conformations.

Again, for practical purposes, software such as the WinGPC Software automatically determines the conformational averages $\langle R_g^2 \rangle_i$ for each chromatographic slice, since those can be considered as monodisperse. The overall elugram average size is then the z-average of the squared

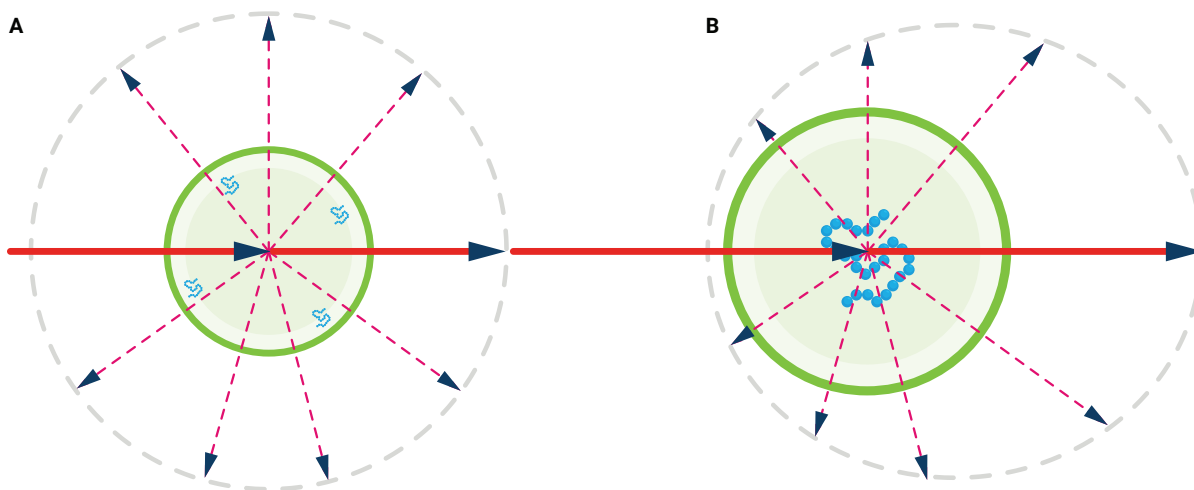


Figure 2. Scattering intensity distribution of an isotropic scatterer (A) and of a scattering molecule with $d > \lambda/20$ (B).

radius of gyration. This size is considered from a center of mass-based coordinate system according to Equation 5 and naturally differs from the geometric or microscopic radius R . Calculations of those can be found in literature.⁴

$$\langle R_g^2 \rangle_i = \frac{\sum_j m_j r_j^2}{\sum_j m_j}$$

Equation 5.

As mentioned before, series expansion of the particle form factor and use of Guinier approximation $1/(1-x) = 1+x$ in Equation 3 is only valid for $qR \ll 1$. For larger molecules, solutions for the particle form factor depend on their particle topology. For example, scattering intensity of homogeneous spherical particles possess local minima and maxima, depending on the scattering angle according to Equation 6.⁴

$$P(q) = \frac{9}{(qR)^6} [\sin(qR) - qR\cos(qR)]^2$$

Equation 6.

To become independent of the particle form factor $P(q)$, the scattering intensity is extrapolated versus $q \rightarrow 0$, where the particle form factor equals 1.

Agilent InfinityLab GPC/SEC Solutions, including data acquisition by the Agilent 1260 Infinity II Multi-Angle Light Scattering Detector run with WinGPC Software, can do this extrapolation precisely, as 20 scattering angle plots can be acquired and then processed.

Further, the range of scattering angles is of great importance. Since the q -vector scales as an inverse length scale, resolution becomes better at higher angles and more details such as conformational changes are seen. In contrast, a more reliable mass information (a particle form factor-independent scattering intensity) is given at small angles in good approximation. The 1260 Infinity II Multi-Angle Light Scattering Detector spans a wide range of 20 angles from 12° up to 164°. Especially in the small angle region, the 1260 Infinity II Multi-Angle Light Scattering Detector offers three more angles of 12°, 20°, and 28°, making molar mass determination more accurate.

An issue faced with some light scattering detector types is the cell design, resulting in correction terms due to changing refractive indices at the liquid/glass interface. In the 1260 Infinity II Multi-Angle Light Scattering Detector, this is circumvented by placing the photodiodes planar on the cylindrical glass cell, so that the detector angle equals the scattering angle. Further, by the design of the cell, scattering

contributions from contaminations such as dust are reduced, making the signals less noisy. With a red wavelength 660 nm 120 mW laser diode, the detector also has enough power for weakly scattering samples. Figure 3 shows the LS trace chromatogram of the monoclonal antibody bevacizumab primary structure on a mAb SiO₂ 3 μm analytical column in PBS buffer. The results of the corresponding slice-wise Zimm plots given by 20 angles for each chromatographic slice yields the molar mass fit given in Figure 4. By this technique, it is possible to deduce the true molar mass of 147 kDa with only approximately a 1% deviation from the literature.⁷ The radius of gyration for the primary structure of bevacizumab yields $\langle R_g \rangle_z = 11$ nm.

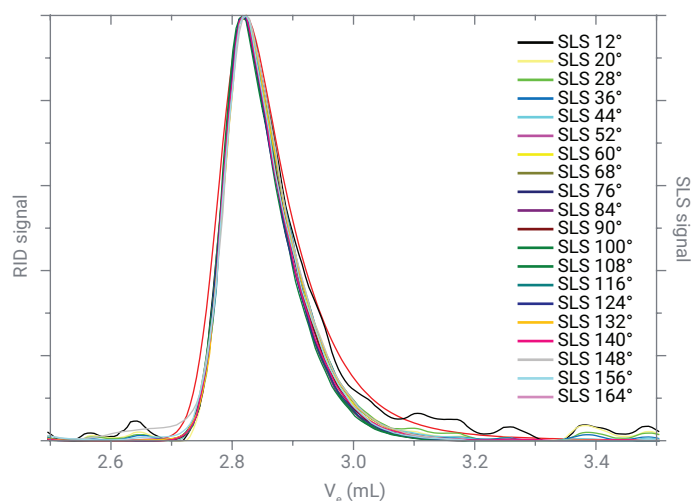


Figure 3. Light scattering intensities of 20 angles of 5 g/L bevacizumab on a mAb SiO₂ 3 μm microbore column in 34 mM PBS + 0.3 M NaCl.

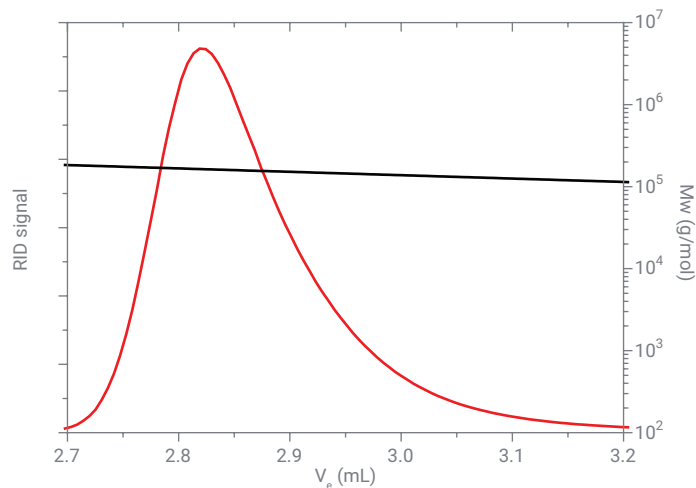


Figure 4. Molar mass fit of bevacizumab elugram from light scattering detector with Mw = 147 kDa.

Dynamic light scattering (DLS) in SEC

For molecules ranging from 1 nm up to micrometers in size, dynamic light scattering (DLS) can also be a good choice for size determination. Generally, DLS spans a much wider range in size determination than SLS from a few nanometers to the micrometer scale. The sizes (the hydrodynamic radius R_H) are calculated from the diffusion coefficient D of the molecule due to its Brownian motion. R_H is then given by the Stokes-Einstein equation (Equation 7).

$$D = \frac{kT}{6\pi\eta R_H}$$

Equation 7.

According to Einstein's law of the movement of dispersed particles in quiescent liquids, R_H is considered the radius of an equivalent sphere.⁸ In the simplest form for monodisperse hard spheres, the diffusion coefficient D is part of a relaxation time $\tau = 1/Dq^2$ with the scattering vector q of a normalized single-exponential decaying function $g_1(t)$, which is given by comparing two scattering intensities each after certain incremental time intervals Δt respectively, which are averaged over the whole correlator run time for each correlator channel according to Equation 8 with A the baseline (the scattering intensity correlation for $t \rightarrow \infty$, $\langle I(q,t) \rangle^2$).^{4,6}

$$g_2(t) - 1 = \frac{\langle I(q,t)I(q,t + \Delta t) \rangle - A}{A} = g_1(t)^2 = \exp(-2t/\tau)$$

Equation 8.

The rightmost term of Equation 8 is also called dynamic structure factor squared. Figure 5 shows the normalized autocorrelation function of an SEC-fractionated immunoglobulin G (IgG) primary structure with $R_H = 6$ nm and a higher associate of $R_H = 11$ nm.

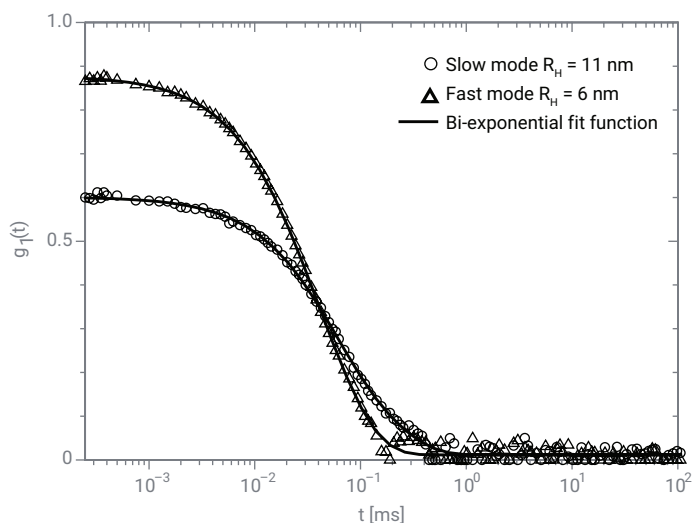


Figure 5. Single autocorrelation functions of SEC-separated IgG fractions of $R_H = 6$ nm (fast mode) and $R_H = 11$ nm (slow mode).

As mentioned earlier, this simple equation is only valid for monodisperse hard spheres. For nonmonodisperse or nonspherical polymers^{9,10}, the dynamic structure factor can be expressed as the sum of single mono-exponential decay functions i , weighted by its scattering intensity contribution, which depends on the particle number density n_i , molar mass M_i , and particle form factor $P_i(q)$,⁴ so one gets Equation 9.¹

$$g_1(t) = \frac{\sum_i n_i M_i^2 P_i(q) g_{1,i}(t)}{\sum_i n_i M_i^2 P_i(q)}$$

Equation 9.

For simplicity, one can rewrite the equation as shown in Equation 10.⁶

$$g_1(t) = \sum_{i=1}^m a_i \exp(-t/\tau_i)$$

Equation 10.

Equation 10 can be solved in the form of a series expansion taking logarithm of $g_1(t)$ with the first cumulant being the average diffusion coefficient at a fixed scattering vector.⁴ For most broad monomodal correlation functions, a bi-exponential fitting approach with $m = 2$ is fully sufficient.¹ Since for each molar mass M_i we find a diffusion coefficient D_i , the average diffusion coefficient can be defined as shown in Equation 11.

$$\langle D_{app}(q) \rangle = \frac{\sum_i n_i M_i^2 P_i(q) D_i}{\sum_i n_i M_i^2 P_i(q)}$$

Equation 11.

Since for polydisperse samples the dynamic structure factor $g_1(t)$ as well as the apparent diffusion coefficient $D_{app}(q)$ become q -dependent due to polydispersity or internal segmental or rotational modes of motion, $D_{app}(q)$ must be extrapolated for $q \rightarrow 0$. In this limit, the apparent diffusion coefficient becomes a z -average according to Equation 12,¹ where the particle form factor also equals $P_i(q) = 1$ and neither segment fluctuations nor rotational terms must be considered.

$$\langle D \rangle_z = \lim_{q \rightarrow 0} \langle D_{app}(q) \rangle = \frac{\sum_i n_i M_i^2 D_i}{\sum_i n_i M_i^2}$$

Equation 12.

According to Stokes-Einstein, we get the z -average of the inverse hydrodynamic radius $\langle R_H^{-1} \rangle_z$. The angular dependency of the diffusion coefficient becomes relevant for particles larger than $R_H > 20$ nm.¹ Most particle sizers that can be used as online instruments are designed as single angle machines (sla-DLS). Typically, correlation is performed on the 90° static light scattering signal. Since in SEC molecules are separated by size, a mono-exponential decay function can be assumed for each slice. Nevertheless, the scattering contribution of segmental or rotational modes of motion can also become relevant for isotropic flexible polymers or anisotropic particles larger than 20 nm. Only at small qR -regimes, those terms can be neglected. One option to circumvent this problem is to measure at low scattering angle, for instance $\theta = 15^\circ$, where one gets true molar masses and diffusion coefficients. In the presence of larger particle fractions, which in SEC can sometimes be caused by column bleeding or dust particles, smaller fractions are unseen due to the molar mass weighted scattering intensity. With increasing scattering angle, particle form factor may decay first for larger particles, so that the scattering contribution decreases in favor of smaller particle fractions. The dual angle dynamic light scattering detector (LSD) ($\theta = 15^\circ$ and 90°) offered with the Agilent 1260 Infinity II Bio-SEC Multidetector System takes $\theta = 90^\circ$ as a good compromise for collecting correlation data. The results for that correlation hold true with only moderate deviation for flexible biomolecules in size range of $R_H < 40$ nm or hard spheres independent of size.¹

It is important to note that dynamic light scattering yields diffusion coefficients from which sizes are calculated. It provides no information about molar mass—this is only done by static light scattering.

Often, biomolecules, including LNP, are more heterogeneous and larger in size, so angular dependency arises. For those molecules, only apparent diffusion coefficients are available,

which are larger than the true z -average, that is, molecules are underestimated in size. This fact must be considered in the size determination of bigger molecules, even when monodispersity due to SEC separation is assumed. Figure 6 shows the 90° light scattering detector signal (purple curve) of bovine serum albumin (BSA), which forms aggregates in 50 mM PBS buffer solution at pH = 7.4.

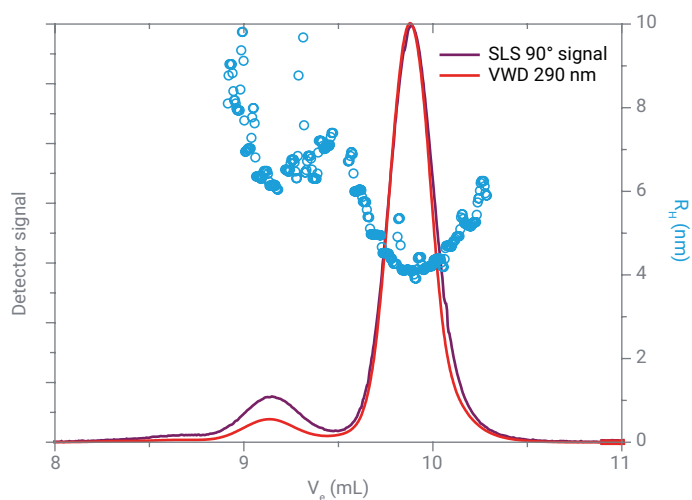


Figure 6. Chromatogram of partially associated bovine serum albumin (BSA) revealed by dynamic light scattering (turquoise curve), UV-Vis signal 280 nm (red curve), and light scattering signal 90° (purple curve).

An advantage for LS is the sensitivity of light scattering detectors compared to UV-Vis detectors due to the molar mass dependency of the scattering intensity.

The primary structure of BSA has a size of $R_H \sim 4$ nm and the associate a size of $R_H \sim 8$ nm, which has been resolved on an Agilent PROTEEMA 300 Å, 5 μ m analytical column in 50 mM PBS buffer. This molecule is considered to be an isotropic scatterer and cannot be conclusively size determined by static light scattering.

Another example is the separation and size determination of higher associates of immunoglobulin G (IgG) from the primary structure ($R_H = 5.5$ nm) on a mAb SiO₂ 3 μ m analytical column. Shown in Figure 7, the R_H curve (turquoise curve) adapts an exponential decaying function over the elution volume V_e , which is in good agreement with theory.¹¹

The relative stronger intensity of the 15° LS signal of the higher associate of IgG ($R_H \sim 8$ nm) in relation to the concentration detector signal is again due to its higher mass contribution. Note that the turquoise curve in Figure 7 is not an intensity curve, but the calculated hydrodynamic radius of the autocorrelator.

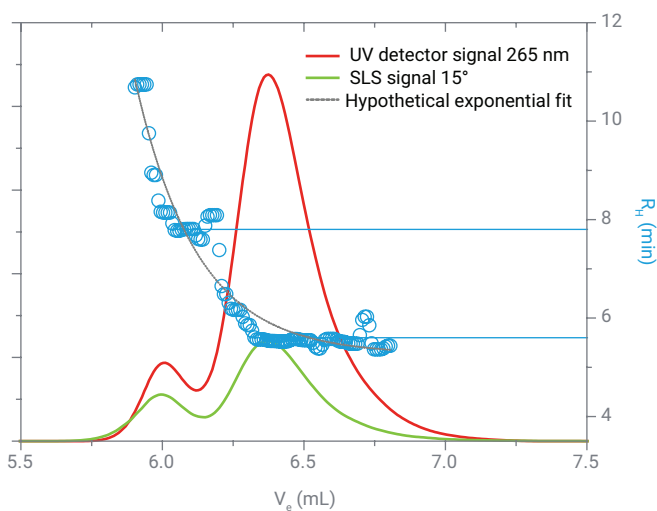


Figure 7. Chromatogram of IgG on a SiO₂ 3 µm analytical column in 34 mM phosphate buffer pH = 6.6 + 0.5 M NaCl with UV signal (red), LS 15° signal (green), and hypothetical exponential fit (gray).

It should be mentioned here that by combination of static and dynamic light scattering, the topology of molecules can be determined by the empirical dimensionless parameter ρ (Equation 13), adapting $\rho = 0.8$ for homogeneous spheres and $\rho = 1.5$ for random polymer coils.⁴

$$\rho = \frac{R_g}{R_H}$$

Equation 13.

This topological information can also be extracted online. Figure 8 shows the chromatogram of thyroglobulin in 10 mM PBS buffer at pH = 7.4. For this measurement, a concentration detector (VWD) was combined with the 20-angle 1260 Infinity II Multi-Angle Light Scattering Detector and a dynamic light scattering detector (the 1260 Infinity II Bio-SEC Multidetector System). The higher molar mass fractions of associated thyroglobulin at lower elution volume are more pronounced in the light scattering signal due to molar mass dependency. The radius of gyration for each slice in the chromatogram was detected by a 20-angle Zimm plot at a known concentration each. That is why the R_g plot is limited to the range where the intensity of the concentration detector is high enough, despite a strong light scattering signal. In contrast, the reliability of the hydrodynamic results is better for a higher dilution of an undisturbed diffusion process. The R_H plot spans a much broader range due to independency of the concentration signal at lower elution volumes and a clearly extended size range to smaller sizes at higher elution volumes. For the primary structure of thyroglobulin, one gets $R_g = 12$ nm and $R_H = 9$ nm, for the higher associate $R_g = 16$ nm and $R_H = 14$ nm. By combining both curves (R_g/R_H), changes

in topology can be detected along the chromatogram (ρ -ratio, blue curve). In the context of SEC, DLS provides a robust and easy alternative to calibrate the column system universally by plotting $\log V_H$ versus elution volume V_e , which should be a universal linear decaying function independent of the respective polymer-solvent combination.⁴ The only prerequisite is a nonenthalpic SEC separation mechanism.

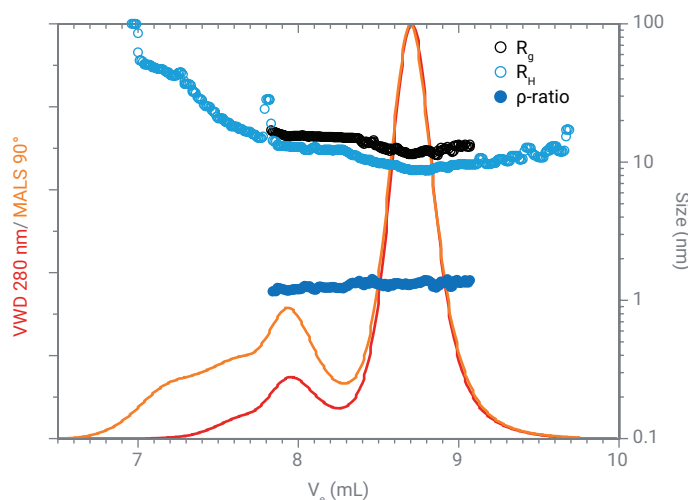


Figure 8. Chromatogram of thyroglobulin on an Agilent PROTEEMA 300 Å, 5 µm analytical column in 10 mM PBS pH = 7.4 equipped with static and dynamic light scattering detectors.

Conclusion

Light scattering technique, static (SLS) and dynamic (DLS) or the combination of both, is a powerful and robust tool to get information about molar mass, size, and topology of any biomolecule of interest. Following size separation by SEC, size fractions can be measured individually, making a precise analysis of the respective biological sample possible. By the 20 angles of the Agilent 1260 Infinity II Multi-Angle Light Scattering Detector, a precise extrapolation towards zero scattering angle is possible, yielding an exact weight average of molar mass and the radius of gyration. By these data (molar mass and radius of gyration), the topology of the molecule can also be analyzed by plotting the logarithm of the radius of gyration versus logarithm of molar mass and getting the topology by the slope in analogy to the Mark-Houwink plot. In Agilent WinGPC Software, it is possible to implement an extra dynamic light scatterer, the Agilent 1260 Infinity II Bio-SEC Multidetector System, to monitor the sizes of the sample fractions. One of the unique strengths of dynamic light scattering in comparison to static light scattering is the much broader size range from 1 to 2 nm up to micrometers and the direct size information obtained in the software. By the combination of the sizes from static and dynamic

light scattering, one can also conclude the topology of the biomolecule associates. Concluding, all this is easily done in a straightforward and precise way only by SEC with the right choice of detector.

References

1. Fischer, K.; Schmidt, M. Pitfalls and Novel Applications of Particle Sizing by Dynamic Light Scattering. *Biomaterials* **2016**, *98*, 79–91.
2. Coffey, A.; Kondaveeti, S. An AdvanceBio HIC Column for Drug-to-Antibody Ratio (DAR) Analysis of Antibody Drug Conjugates (ADCs). *Agilent Technologies application note*, publication number 5994-0149EN, **2018**.
3. Agilent GPC/SEC Standards home page. <https://www.agilent.com/en/product/gpc-sec-columns-standards/gpc-sec-standards> (accessed **2023**).
4. Schärtl, W. Light Scattering from Polymer Solutions and Nanoparticle Dispersions; Springer-Verlag Berlin Heidelberg New York, **2007**.
5. Masuelli, M.; Gassmann, J. Advances in Physicochemical Properties of Biopolymers, Part 1; Bentham Science Publishers: **2017**, pp 28–59.
6. Arndt, K.; Müller, G. Polymercharakterisierung; Carl Hanser Verlag München Wien, **1996**.
7. Hirvonen, L. *et al.* Hydrodynamic Radii of Ranibizumab, Aflibercept and Bevacizumab Measured by Time-Resolved Phosphorescence Anisotropy. *Pharm. Res.* **2016**, *33*, 2025–2032.
8. Einstein, A. Über die von der molekularkinetischen Theorie der Wärme geforderte Bewegung von in ruhenden Flüssigkeiten suspendierten Teilchen. *Ann. Phys.* **1905**, *17*, 549–560.
9. Borsali, R.; Nguyen, H.; Pecora, R. Small-Angle Neutron Scattering and Dynamic Light Scattering from a Polyelectrolyte Solution: DNA. *Macromolecules* **1998**, *31*(5), 1548–1555.
10. Lehner, D.; Lindner, H.; Glatter, O. Determination of the Translational and Rotational Diffusion Coefficients of Rodlike Particles Using Depolarized Dynamic Light Scattering. *Langmuir* **2000**, *16*(4), 1689–1695.
11. Giddings, J. *et al.* Statistical Theory for the Equilibrium Distribution of Rigid Molecules in Inert Porous Networks. Exclusion Chromatography. *J. Phys. Chem.* **1968**, *72*(13), 4397–4408.

www.agilent.com

RA45065.4247800926

This information is subject to change without notice.

© Agilent Technologies, Inc. 2023
Printed in the USA, May 30, 2023
5994-6110EN